Macromolecular Bioscience
www.mbs-journal.de

Preclinical Testing of 3D Printed, Cell Loaded Hydrogel Based Corneal Substitutes on Rabbit Model

*Deniz Basoz, Aslihan Akalinli, Senem Buyuksungur, A. R. Cenk Celebi, Deniz Yucel, Nesrin Hasirci, and Vasif Hasirci**

Many people lose their vision due to corneal stroma injuries of the eye and the golden solution is transplantation of allografts from donors. Unfortunately, the limited availability of donor tissue, risk of disease transmission, and immune rejection are serious handicaps. However, implants made of biomaterials can be used as substitutes. In this study, cell-loaded and cell-free, methacrylated gelatin (GelMA) implants are 3D printed and tested under in vitro conditions. The samples are physically characterized for their printability, equilibrium water content, compressive mechanical strength, and transparency; they retained 60%–80% of light transmission in the visible region as in the native corneas. In brief, they are suitable for further testing. Then cell loaded samples are tested in vivo on New Zealand white rabbits for 90 days. In the in vivo tests, these cell loaded, disk shaped implants are almost completely degraded and allowed reorganization of the tissue forming at the implantation site. Also, the immune response initially observed decreased in time and by the end of 90 days the tissue regained its normal, healthy architecture with multilayered, non-keratinized epithelium. It can be concluded that the implants developed in this study are promising for clinical use in corneal stroma recovery.

1. Introduction

The cornea is a transparent, multilayered structure located at the outermost part of the eye. The functions and light transmission capability of the cornea are achieved by its highly organized structure and mainly the stromal cells existing in its structure. Due to its exposed location in the eye, the cornea is very vulnerable to infection and trauma.[1] Today, the most common cause of blindness after cataracts is corneal damage. Although the cornea appears as a very thin and simple tissue, its structure is very complex, and therefore, it is very difficult to prepare a substitute for it. The stroma, the thickest layer (90%), is the most complex component of the cornea. It consists of ca. 2 µm thick, 200 parallel collagen fiber layers which are positioned at 90° angle to each other in subsequent layers. This micro organization is of vital importance for the mechanical strength and optical properties of the cornea, and any disruption of this structure immediately reflects on its transparency.[2] Keratocytes, which are corneal stroma fibroblastic cells, are organized within this structure and are very important for the preservation of the structure.[3]

Transplantation is the most viable common treatment for corneal damage, but the number of suitable donor corneas available is far below the actual need.[4] Keratoprostheses, which are the only option for transplantation today, are preferred only in cases where tissue rejection or risk is high. These synthetic polymer-based materials can lead to an increase in intraocular pressure and, as a result, formation of glaucoma, which is accompanied by irreversible optic nerve damage.[5,6]

D. Basoz, A. Akalinli, D. Yucel, V. Hasirci
Acibadem Mehmet Ali Aydinlar University (ACU)
Biomaterials R&D Center
Istanbul 34752, Türkiye
E-mail: vasif.hasirci@acibadem.edu.tr

The ORCID identification number(s) for the author(s) of this article can be found under https://doi.org/10.1002/mabi.202400595

DOI: 10.1002/mabi.202400595

D. Basoz, D. Yucel, V. Hasirci
ACU
Graduate Department of Biomaterials
Istanbul 34752, Türkiye

A. Akalinli, V. Hasirci
ACU
Graduate Department of Biomedical Engineering
Istanbul 34752, Türkiye

S. Buyuksungur, N. Hasirci, V. Hasirci
Middle East Technical University (METU)
BIOMATEN
CoE in Biomaterials and Tissue Engineering
Ankara 06800, Türkiye

A. R. C. Celebi
ACU
School of Medicine
Department of Ophthalmology
Istanbul 34752, Türkiye

Imitating the microorganization of the corneal stroma is the most important requirement for a successful substitute. Although biomaterials in the form of sponges, fibers, and films aiming to imitate the structure of the stroma are reported in the literature, there is no viable corneal equivalent in daily clinical use yet. Some corneal conjugates, which are in Phase 1 in clinical trials, are patternless, flat, and cell-free hydrogels.[7,8]

Other methods used and devices developed are complex, expensive, and cannot adequately mimic the structure and organization of the cornea. In addition, many corneal conjugates found in the literature have disadvantages such as long preparation times, need to culture the cells on the scaffold after its production, and the harmful effects of the chemicals used when stabilizing the structure by crosslinking.[9–11] As a result, the absence of a widely used artificial cornea substitute is still a challenging problem.

There are various natural (e.g., gelatin,[12,13] collagen,[14,15] chitosan,[10,16] hyaluronic acid[17,18]) and synthetic (e.g., PEG,[19,20] PVA[21,22]) hydrogels studied as cornea substitutes. The reliability of a modified natural material, gelatin, has been demonstrated by many research groups for various tissues.[23–25] Methacrylated gelatin (GelMA) was used in our earlier studies in the construction of the corneal stroma layers and successful results were obtained in in vitro studies. This was especially because they had good mechanical properties, high light transmittance and cell viability, and extracellular matrix proteins such as collagen type I and V produced by the cells.[12,26] The suitability of cell-free GelMA hydrogel slabs as corneal stroma substitutes were demonstrated by an in vivo study conducted with 2 rabbits.[27] In that pilot study carried out by our group, it was observed that the transparency of the eye was preserved for the whole duration of 100 days with no signs of incompatibility (dry eye, vascularization, etc.).

Three-dimensional printing (3DP) is a widely used production method developed in the last decades. It enables the production of patient-specific medical devices with controlled size, shape, and porosity. 3DP tissue engineered devices are not many.[28] Only a few groups have studied and published on this subject.[14,29–32]

3D Bioprinting (3DBP) enables the researchers to mimic the orthogonal organization of the stromal layers and keratocytes of the native eye by printing orthogonally organized struts carrying the cells. 3D Bioprinting also enables us to prepare implants in a patient specific fashion. 3DP hydrogels loaded with cells, in addition to creating a highly controlled internal and external architecture, also provide orthogonal organization of keratocytes similar to that in the original stroma. This organization is also critical for the light transmission capability of the cornea.

In the present study, hydrogel based implants of GelMA, were prepared with the 3DP technique both in cell-free and cell-loaded states, and only the cell-loaded implants were tested as corneal stroma substitutes in vivo. Cell-loaded 3DP GelMA hydrogels were prepared by the introduction of human keratocytes into the orthogonally organized gel. The suitability and effectiveness of these corneal stroma implants were studied under in situ, in vitro, and in vivo conditions.

This in vivo study showed the compatibility of the cell loaded 3DP stroma equivalents through long term studies. Immunostaining displayed regular lamellar stroma structure with parallel collagen fibers. Keratocytes were found in and around the implant. These implants mimic the micro-level organization of the stroma with its keratocytes organized in accordance with the natural internal structure of the stroma, and therefore, have a high potential for clinical application.

2. Results and Discussion

2.1. Determination of Degree of Methacrylation of GelMA Polymer with ^{1}H-NMR Analysis

The degree of methacrylation (DM) is defined as the ratio of methacryl groups attached to the amine groups of the amino acid lysine of gelatin to the original amine lysine groups in the pristine gelatin before the reaction. DM was found as 88%, indicating a higher efficiency of methacrylation than some other studies in the literature (**Figure 1A**).[12,31]

2.2. Printing of Cell-Free GelMA Hydrogels

3D model was printed and then cut using a 4 mm sterile punch for in vivo studies. Figure 1B shows a 3D printed GelMA after swelling in PBS (10 mM, pH 7.4) overnight at 37 °C, and the freeze-dried form. The intended grid structure was successfully created through the 3DP process.

2.3. Characterization of Implants

2.3.1. Equilibrium Water Content of 3DP Hydrogels

Equilibrium water content (EWC) of cell free GelMA hydrogels were calculated separately for both environments by incubating them in PBS (10 mM, pH 7.4) and distilled water at 37 °C for 24 h. The EWC of the hydrogels were found to be 93 ± 2% in PBS and 97 ± 1% in distilled water. This value is higher than 3D printed implants (85%) published by Zhang et al.[32]

2.3.2. Enzymatic Degradation of 3DP GelMA Hydrogels

It is observed that under collagenase-II accelerated degradation conditions, GelMA lost 55% of its weight in 2 h, while the Control group (enzyme free, PBS only) reveals 2% loss in the same

D. Yucel
ACU
School of Medicine
Department of Histology and Embryology
Istanbul 34752, Türkiye
N. Hasirci
METU
Department of Chemistry
Ankara 06800, Türkiye
N. Hasirci
Near East University
Department of Bioengineering
TRNC
Mersin 10 99138, Türkiye

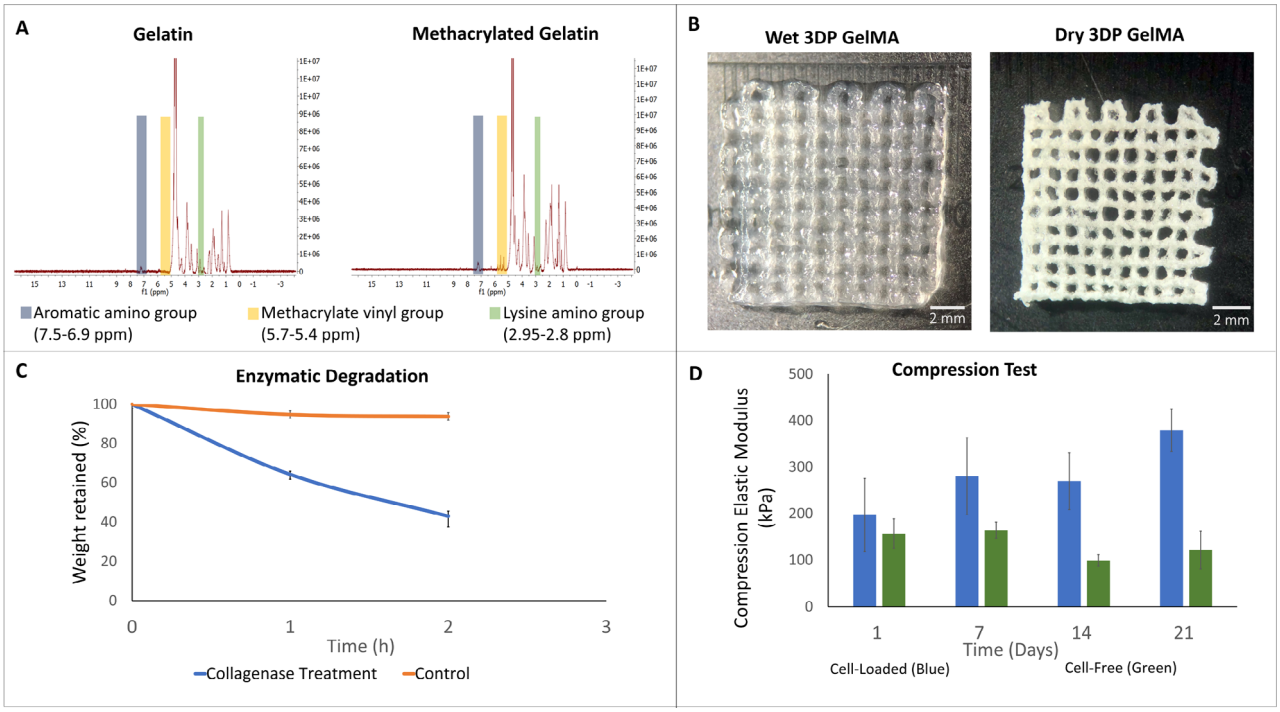

Figure 1. Properties of GelMA hydrogels and pristine gelatin. A) ^{1}H-NMR spectra of pristine gelatin and methacrylated gelatin (GelMA polymer) used in the calculation of methacrylation degree of gelatin (phenylalanine (7.5–6.9 ppm), methacrylated vinyl (5.7–5.4 ppm), lysine (2.95–2.8); B) 3D printed GelMA hydrogels in wet and dry state; C) c Degradation of collagenase treated and untreated (control) GelMA implants. D) Compression test results of cell-free and cell-loaded 3DP GelMA hydrogels.

period (Figure 1C). A GelMA implant studied under comparable enzymatic conditions was reported to present a similar level of enzymatic degradation (ca. 55%).[32] These indicate that under in vivo conditions where enzymes will be present, GelMA based hydrogels will in the long term be completely degraded and substituted by the regenerated tissue.

2.3.3. Mechanical Properties of Cell-Free and Cell-Loaded GelMA Hydrogels

The mechanical properties of cell-free and cell-loaded GelMA hydrogels were determined by compression mechanical testing. Compressive elastic modulus of the cell free and cell loaded samples were calculated from the slope of the first region of the stress-strain plots, and found to be on average 136 kPa for cell free and, 281 kPa, for cell loaded samples (Figure 1D). The interesting observation is that while the cell free sample does not show a trend, the mechanical property of the cell loaded samples kept increasing with time. This increase over time is probably due to cellular activity leading to the production of an extracellular matrix within the hydrogel as reported by our group earlier.[31]

2.3.4. Light Transmittance of Corneal Implants

Stereomicroscopic images of cell-loaded and cell-free hydrogels are presented in **Figure** 2A. According to the literature, cornea transmits radiation from 300 nm in the UV to 2500 nm in the infrared region.[33,34] The total transmittance increases rapidly from 300 nm and reaches to 80% at 380 nm, and from 500 to 1300 nm is greater than 90 percent. Our studies with native rabbit cornea revealed a similar behavior between 200 and 700 nm (Figure 2B)

The light transmittance of the cell-loaded and cell-free samples prepared in this study were measured in the range 250–700 nm with UV–Vis spectroscopy and showed that at 300 nm transmission is almost zero and rises rapidly to 60% 400 nm and 70% 700 nm (Figure 2C). This high transmittance in the visible region was maintained for the whole 21 day test period regardless of the presence or absence of cells. This practically is the same with that of native cornea. In a study with cell-loaded and cell-free GelMA implants light transmission was studied in the range 400–800 nm and showed an increase from 400 to 700 nm like in the present study but a significant decrease in the transmission of light was observed in this range.[32] It is important that the presence of cells do not significantly decrease the transparency of the implants in time indicating that the patient will have a proper vision from the very beginning of the post-implantation period. Also, the low transmittance in the UV range will protect the implant and the patient from the damaging effects of the radiation.

2.4. In Vitro Studies

2.4.1. Characterization of Human Keratocytes

Flow Cytometry: Surface markers specific for human keratocyte cells (passage 13) were studied using flow cytometry (**Figure** 3). The histograms obtained indicate that the cells exhibit

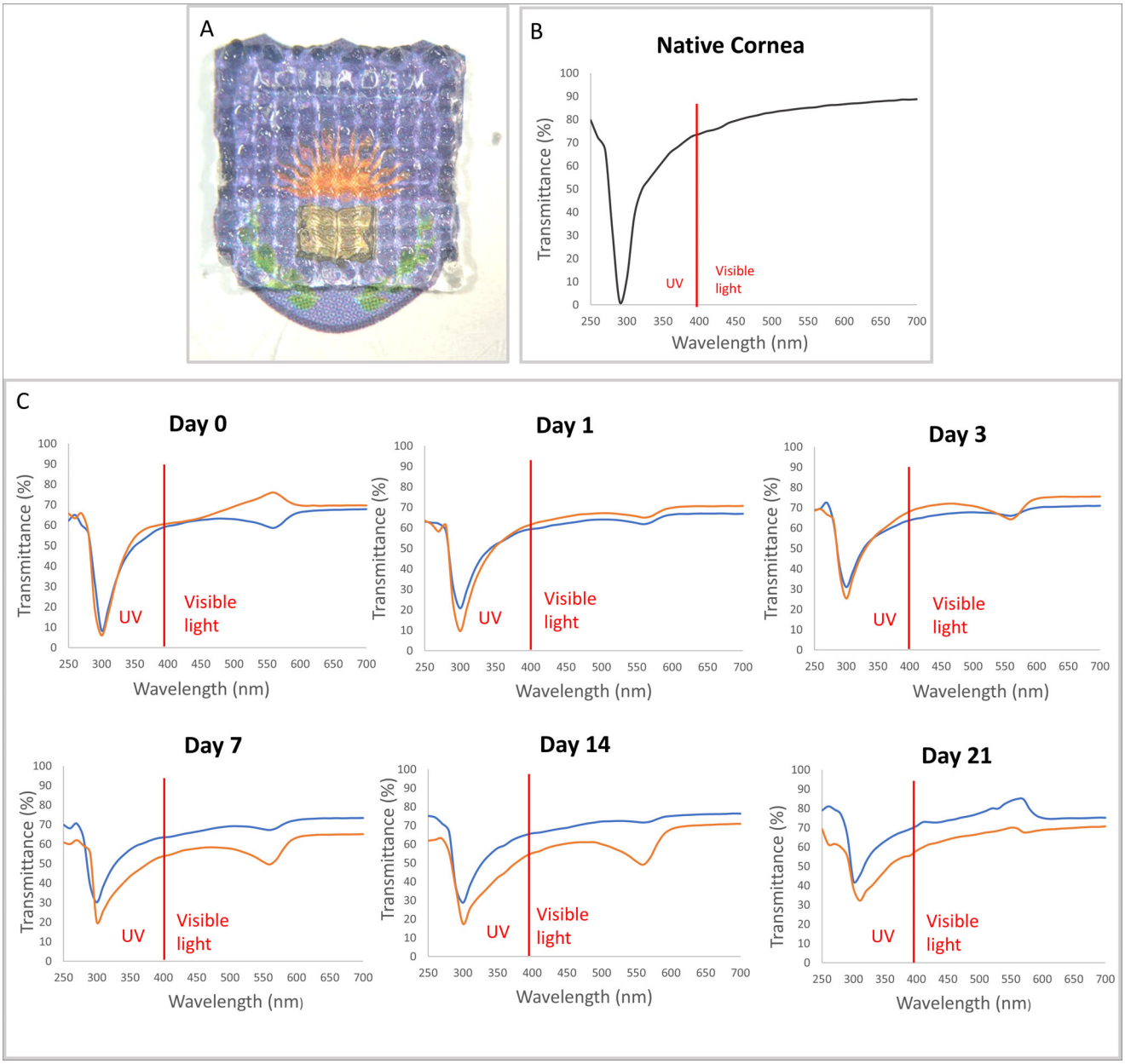

Figure 2. Transmittance of cell-free (orange) and cell-loaded (blue) hydrogels in the 250–700 nm range. A) Stereomicroscopy image of the 3DP hydrogel, B) Light transmittance of the native cornea, C) Light transmittance of 3DP GelMA.

positive expression for CD73 (80.2%) and CD105 (56.6%) which are associated with mesenchymal stem cells. As expected CD34 and CD45, which are not typically found in corneal keratocytes, were negative, with only 1% positivity for CD34 and 0.3% for CD45.

In order to validate the specificity of antibody binding, unstained cells and isotype controls were also analyzed. Both controls exhibited minimal fluorescence, with 99.8% and 99.9% of cells falling in the negative region for the FL1 (Alexa Fluor 488) and FL4 (Alexa Fluor 647) channels, respectively. This overlap with the negative region shows the absence of non-specific binding.

As a result, the isolated keratocyte cells were shown to display the expected surface marker profile, with positivity for CD73 and CD105 and negativity for CD34 and CD45, and confirm the suitability of these keratocytes for use in this study.

Immunocytochemistry: ALDH1A1 is a phenotypic marker, also known to contribute to the protective and refractive properties of the cornea. Lumican is a protein belonging to the keratan sulfate proteoglycan family found in the corneal stroma and is necessary for the light transmission of the cornea. Immunocytochemistry studies of cells was conducted for these proteins found in human keratocytes using confocal laser scanning microscopy (CLSM, Zeiss) to show that the

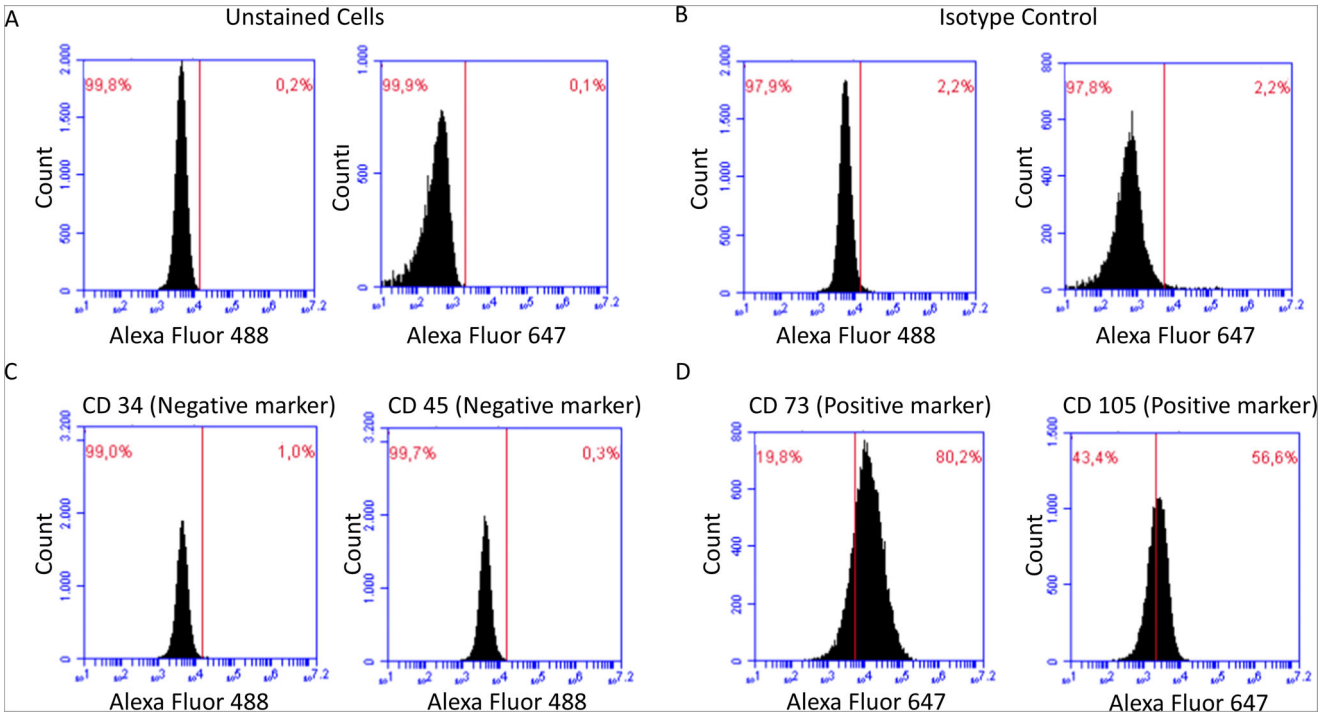

Figure 3. Histograms of flow cytometry results for different antigen expressions: A) Unstained cells, B) Isotype controls, C) Negative expression of CD34 and CD45, D) Positive expression of CD73 and CD105.

cells loaded into the corneal mimic are keratocytes. **Figure 4** shows the expression of ALDH1A1 and lumican by the cells loaded into the 3DBP implants proving their keratocyte nature.

2.4.2. Cell Viability after 3DBP

The viability of the keratocytes loaded into 3DBP GelMA hydrogels was assessed with Live-Dead assay on days 1, 7, 14, and 21.

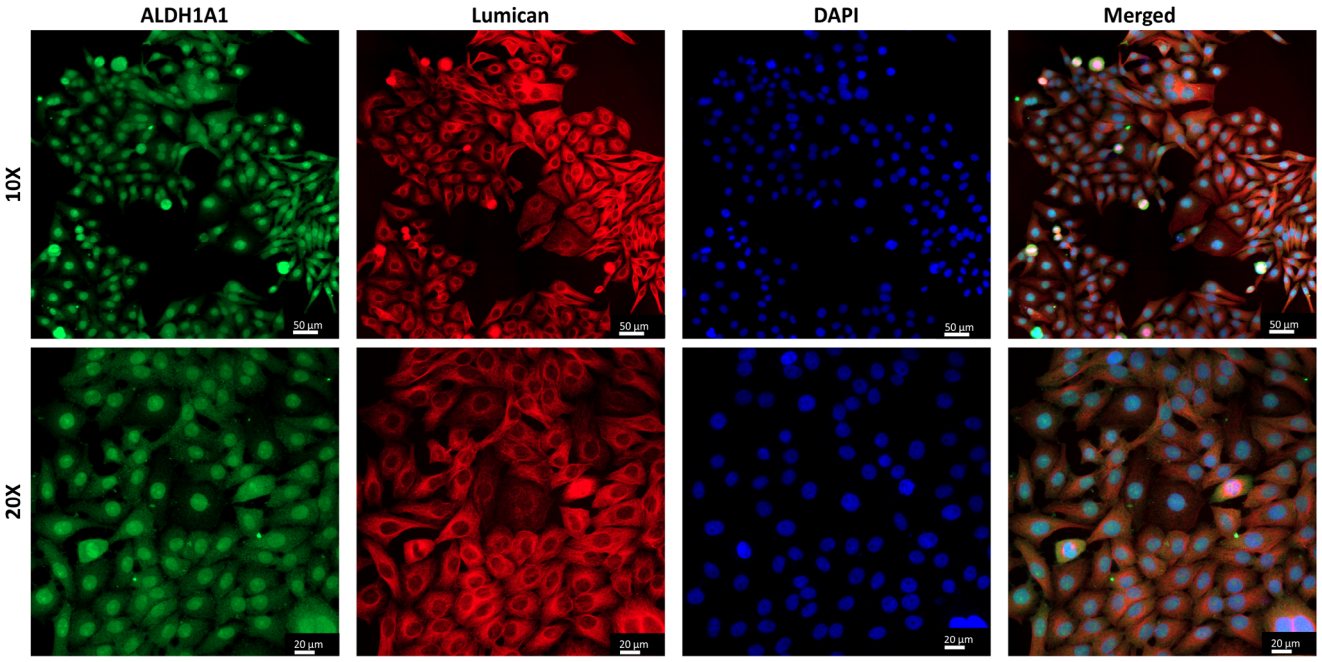

Figure 4. Expression of ALDH1A1 (green) and lumican (red) by the human keratocytes (Passage 13) and DAPI (blue) showing the cell nuclei after immunostaining.

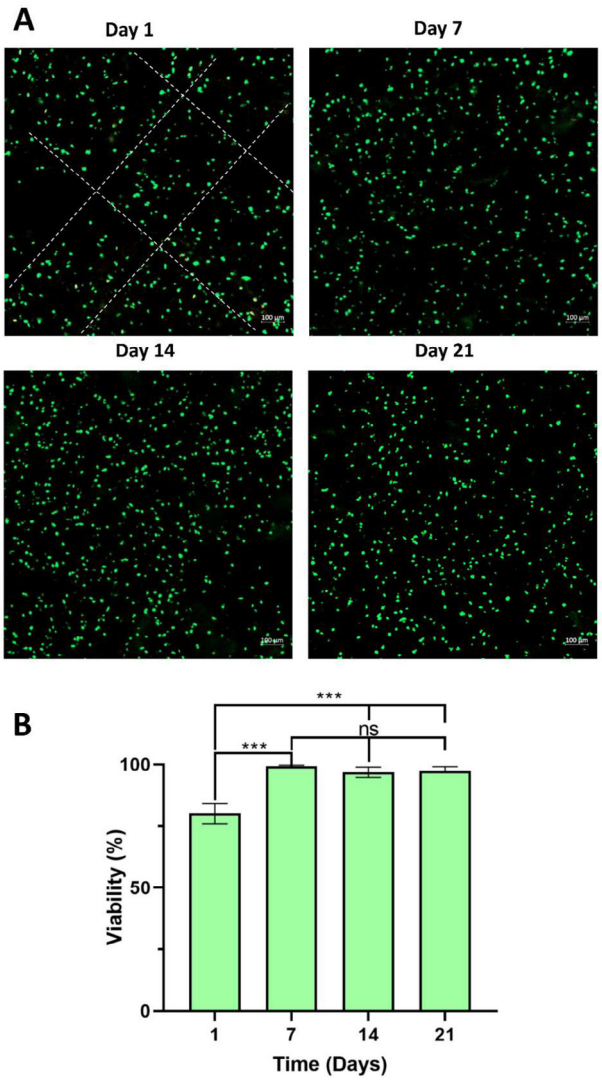

Figure 5. Viability of cells loaded in the 3DP GelMA. A) CLSM of Live-Dead Cell Viability test for days 1, 7, 14, and 21 after printing. The dotted lines indicate the struts of the GelMA implant. Live cells: Green (stained with Calcein AM), Dead cells: Red (stained with ethidium homodimer-1). B) Viability versus Time graph plotted with quantitative results of Live-Dead assay images obtained with NIH ImageJ.

The results show that the viability of keratocytes loaded in the 3DBP GelMA hydrogels on day 1 was ≈80%, and this increased to and stayed as 95% for up to 21 days showing that the preparation and culture conditions were very suitable for the keratocyte survival and performance (**Figure 5**). In a study by Kessler et al.,[32] where methacrylated gelatin/hyaluronan hydrogel was considered for use as carrier for adipose derived stem cells, the cell viability within the hydrogel was ≈80% for 10% hydrogel and 87% for 5% GelMA after the same duration, 21 days of culture, while Zhang et al. (2023)[35] had a quite low viability on day 1 after printing but recovered to ≈80%, later. These are quite comparable to the values obtained in the present study and are acceptable considering the added stress of the 3D printing process on the cells.

2.5. In Vivo Studies

2.5.1. Post Operational Examination of the Rabbit Eyes

Post-implantation, the rabbits were regularly monitored, weekly for the first month, then biweekly, for signs of edema, vascularization, ulcers, inflammation and infection, wound status, rejection, implant color, and position. Fluorescein staining and Schirmer's test were conducted to evaluate tear film regeneration and the damages to the cornea by the incision process.

In the Control group (no surgical procedure) no significant changes were observed.

In the sham group (only lamellar incision), the incision was well tolerated, and minimal vascularization and proper regeneration of the incision site were observed.

In the cell-loaded group (3DBP with keratocytes), the responses were not as simple as the first two groups. It was observed that the implants remained in place until significant degration in the later weeks (**Figure 6**A). On the 3rd week some vascularization and infection were detected. The group was then treated with Moxidexa (active ingredients moxifloxacin and dexamethasone) for one month after which the infection significantly decreased, and vascularization was reduced. During weeks 6–8, most implants underwent considerable degradation, and 4 out of 6 samples were almost completely degraded by week 12. However, no ulceration or edema was observed during this time and Schirmer's test showed no significant differences in tear production among all groups (Figure 6B), and sodium fluorescein (NaF) staining revealed no changes in corneal integrity. The Schirmer's test score is determined by the length of the moistened area of the strips. A young person normally moistens 15 mm of each paper strip while eyes of 33% of normal elderly persons wet only 10 mm in the same period, 5 min.[36,37]

The Schirmer's test results of the present study show that implant and sham were in the range 16–23 mm/5 min after 12 weeks while the Control group result was 21 mm/5 min, showing that the implantation process did not lead to any drying of the eye due to the presence of the implant.

In a study with clinical application to patients with different ophthalmic problems, cell-free implants of carbodiimide-crosslinked recombinant human collagen type III carrying a network of 2-methacryloyloxyethyl phosphorylcholine (MPC) were used. The Schirmer's test results obtained after 24 months was improved (with the cell-free implant it was 6–16 before treatment and 8–20 after treatment).[8]

As for the appearance of the implant during this whole period, a cloudiness and opaqueness were observed accompanied by inflammation at weeks 4–6. Later, it gradually became more transparent, inflammation subsided and degradation continued (Figure 6A). At the end of 12 weeks, 4 of them were completely degraded and disappeared while one of them was slightly visible and the remaining one was intact

2.5.2. Histopathological Examinations

The cornea tissues were stained with Hematoxylin and Eosin and examined with a light microscope and the images of the samples are given in **Figure 7**. Hematoxylin and Eosin

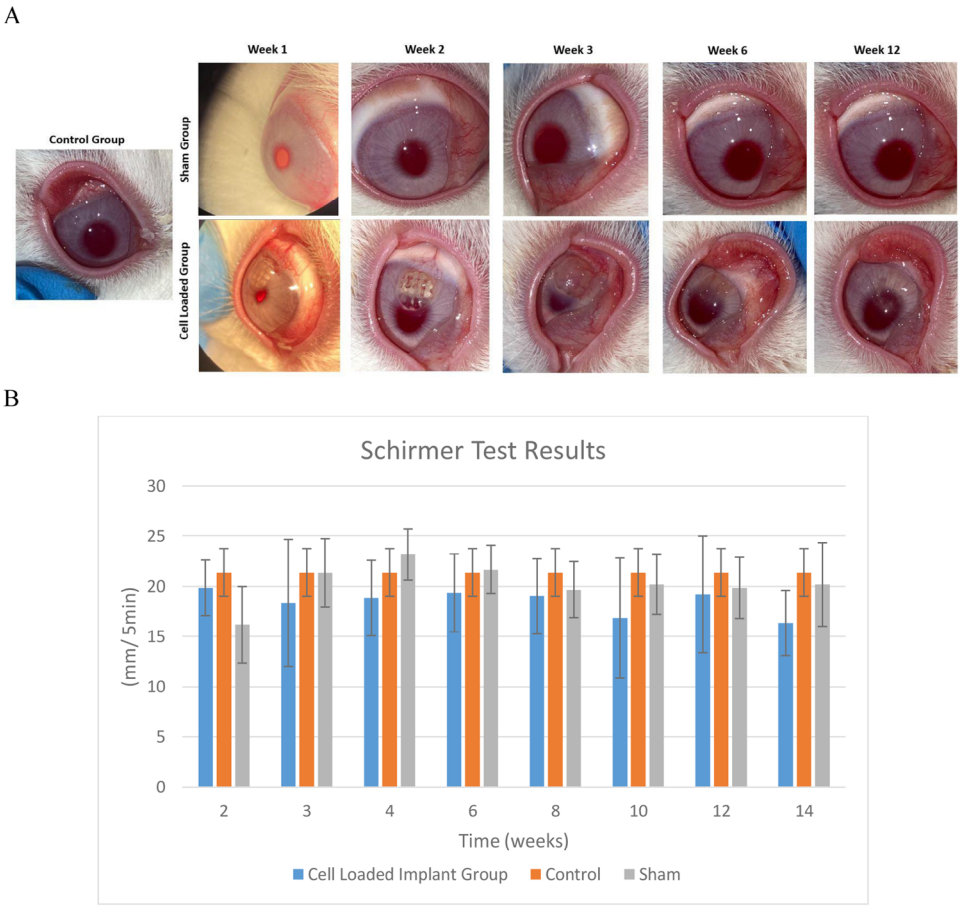

Figure 6. In vivo post-operational results. A) 12 week follow up of Control, Sham, and Cell-loaded implant groups in rabbit eyes, B) Schirmer's test results of Control, Sham, and Cell-loaded Implant groups.

staining was used to evaluate the tissue response and tissue regeneration of corneas after 15 weeks of implantation. In addition, immunostaining was done against collagen type I and collagen type V to assess integration of the implant within the stroma by secretion of ECM molecules (**Figure 8**). The presence of keratocytes around and in the implant was shown with keratocyte-specific marker CD34 (Figure 8). In the corneal tissues of the untreated control group, normal, healthy corneal architecture with multilayered non-keratinized epithelium, lamellar stroma with parallel collagen fibers and single-layer endothelium was demonstrated (Figure 7A). In the sham group, even though an intrastromal pocket was created through a corneal incision as part of a surgical procedure, the pocket area had healed and the stroma tissue exhibited a normal, healthy corneal architecture with lamellar, parallel collagen fibers similar to that of the control group on week 15 (Figure 7B). Moreover, re-epithelialization of the cornea was observed at the incision site, and the single layered endothelium was intact in the sham group.

In the cell-loaded 3DBP implant group, it was observed that the implants had integrated into the host cornea on week 15 (Figure 7C,D). In most of the samples of this group, the implants were almost completely degraded and a significant reduction in the implant size was clearly seen. The implant integration with the host cornea was also reported by Bektas et al. on week 15 using cell-free GelMA hydrogel slabs.[27] A certain level of foreign body reaction after implantation of a biomaterial is expectable and normal during healing process.[38] There was a severe host-immune response in one of the samples (1 out of 6) in which significant inflammatory infiltration was present, the regular lamellar structure was disrupted, and the collagen fibers appeared irregular. In one of the samples, host-immune response was moderate with the presence of inflammatory cell infiltration (Figure 7C). However, the implant was almost completely degraded and the regular lamellar stroma structure with parallel collagen fibers was observed around the implant. The rest of the samples (4 out of 6) were almost completely degraded and exhibited very low immune-inflammatory reaction (Figure 7D). The corneal stroma, displaying a regular lamellar structure was observed in the region where the implant had degraded. Immunohistochemistry studies for collagen types I and V showed that the collagen fibers were parallel especially at the borders as well as on the inside of the implant, a similar observation to the intact stroma at no-implantation region (Figure 8). It indicates that the implant was well integrated with the native tissue and was replaced with new lamellar cornea stroma over time. Upon surgical injury, keratocytes may be converted to myofibroblasts, and when the

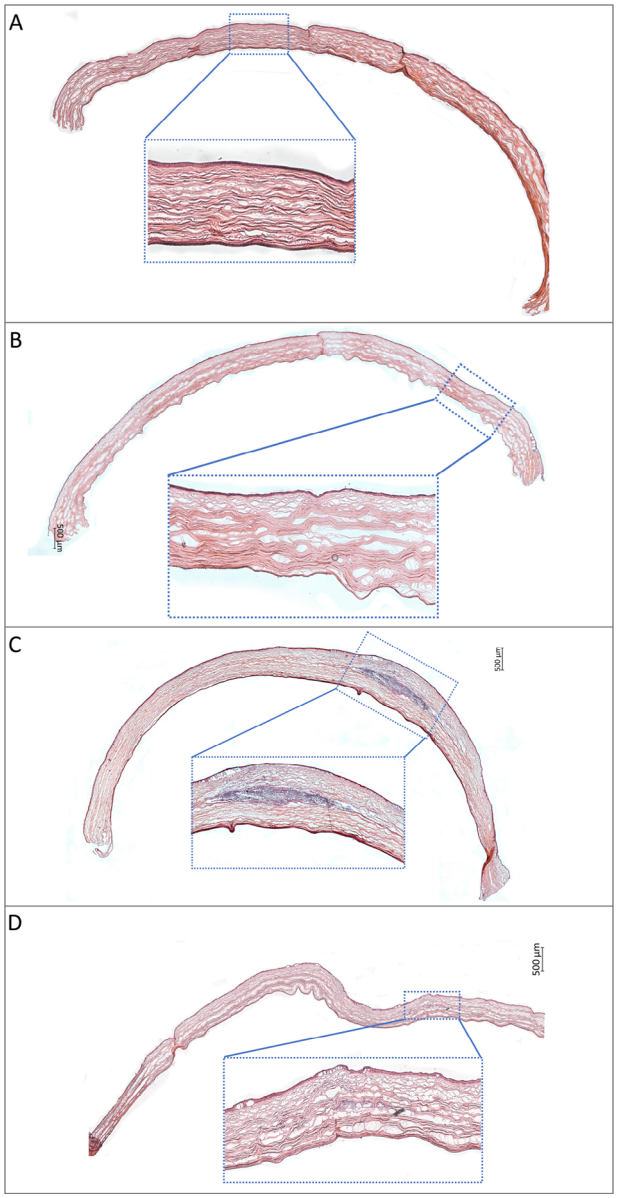

Figure 7. Hematoxylin and Eosin stained sections of the rabbit cornea after 12 weeks of implantation. A) Control group, B) Sham group. Cell-loaded 3DBP GelMA implant groups with C) moderate, and D) low host immune response. Images were captured using the tile method at 10x magnification. Scale bars: 500 µm.

myofibroblast population becomes dominant, their secretions lead to scar tissue formation similar to reports present in literature.[39] In the implant region, the expression of the keratocyte marker CD34 indicated that keratocytes preserved their phenotype and flat morphology, distributing uniformly in the stroma surrounding the remaining implant as well as lodging on the inside (Figure 8). The results of H&E staining and immunohistochemistry demonstrated that the corneal tissue regained its normal, healthy architecture, including the regenerated, multilayered, non-keratinized epithelium, after 15 weeks of cell-loaded 3DBP implantation.

3. Conclusion

The aim of this study was to produce and study the performance of corneal stroma implants in the form of 3D printed GelMA hydrogels with the ultimate goal of using in pilot clinical applications as a solution for the shortage of donor corneas.

The major novelty of the study was the use of 3D printing as a method of implant production. This approach enabled us to mimic the orthogonal alignment of the successive lamelles of the natural corneal stroma. The method was rapid, implants could conveniently be produced with the desired internal and external physical properties and shape, in addition to the material used in the study was biological origin, biodegradable, and could be successfully sterilized by various approaches including gamma irradiation.

The implant material, GelMA, was found to be a suitable biomaterial for in vivo applications, as many other studies have shown, demonstrating transparency, mechanical stability, and reproducible production. In vivo observations revealed that the implant did not cause dry eye, led to minimal or no edema, no ulcer formation in most samples. When the implants loaded with cells were made it was found that neither the cell viability nor the light transmission in the visible range deteriorate. The immunohistochemistry results indicated tissue reorganization after the intervention while the implant degraded gradually to vacate the implantation site for the recovery of the tissue. The implants fully degraded within the 90 day test duration, allowed initiation of recovery of the stroma with parallel collagen fibers organized in a lamellar structure. The foreign body reactions observed were mostly mild. The use of cells specific for the corneal tissue, a key feature of tissue engineering, was apparently influential in accelerating the healing process.

The most important advantage of this implant type is that vision will be gained immediately, the moment the implant is placed in the eye and eventually be replaced by the regenerating tissue leaving no foreign material in the body.

It is, therefore, believed that this tissue engineered 3DBP corneal stroma implant is a very good candidate for testing in pilot clinical studies.

4. Experimental Section

Synthesis of Methacrylated Gelatin (GelMA) Polymer: In this study type A porcine gelatin (80–120 g Bloom, Type A) from Sigma–Aldrich was reacted with methacrylic anhydride to obtain the methacrylated gelatin, which was then treated with UV during the printing process to form the hydrogel GelMA according to the method given in literature.[40] Briefly, Type A porcine gelatin was dissolved in isotonic phosphate buffer (PBS, 10 mM, pH 7.4) to 10% (w/v) at 60 °C. Then, methacrylic anhydride (MA) was added (at a rate of 0.5 mL min^{-1}; 20% (v/v) in the final solution), and the mixture was allowed to react at 50 °C for 1 h. Later, PBS was added (5 times of the volume) to stop the reaction at 40 °C. The resulting solution was dialyzed in 40 °C against distilled water for 1 week to remove excess unreacted methacrylic anhydride. The solution was lyophilized, the GelMA polymer obtained was dried and stored at +4 °C until use.

Methacrylation Degree of GelMA by ^{1}H-NMR Analysis: Unreacted pure gelatin (Gel) and methacrylated gelatin (GelMA) were dissolved (30 mg mL^{-1}) in deuterium oxide (D_2O) at 40 °C. ^{1}H-NMR spectra of the solutions were obtained with a Bruker DPX 400 spectrometer at a frequency of 400 MHz. The ratio of methacrylated groups bound to gelatin (degree of

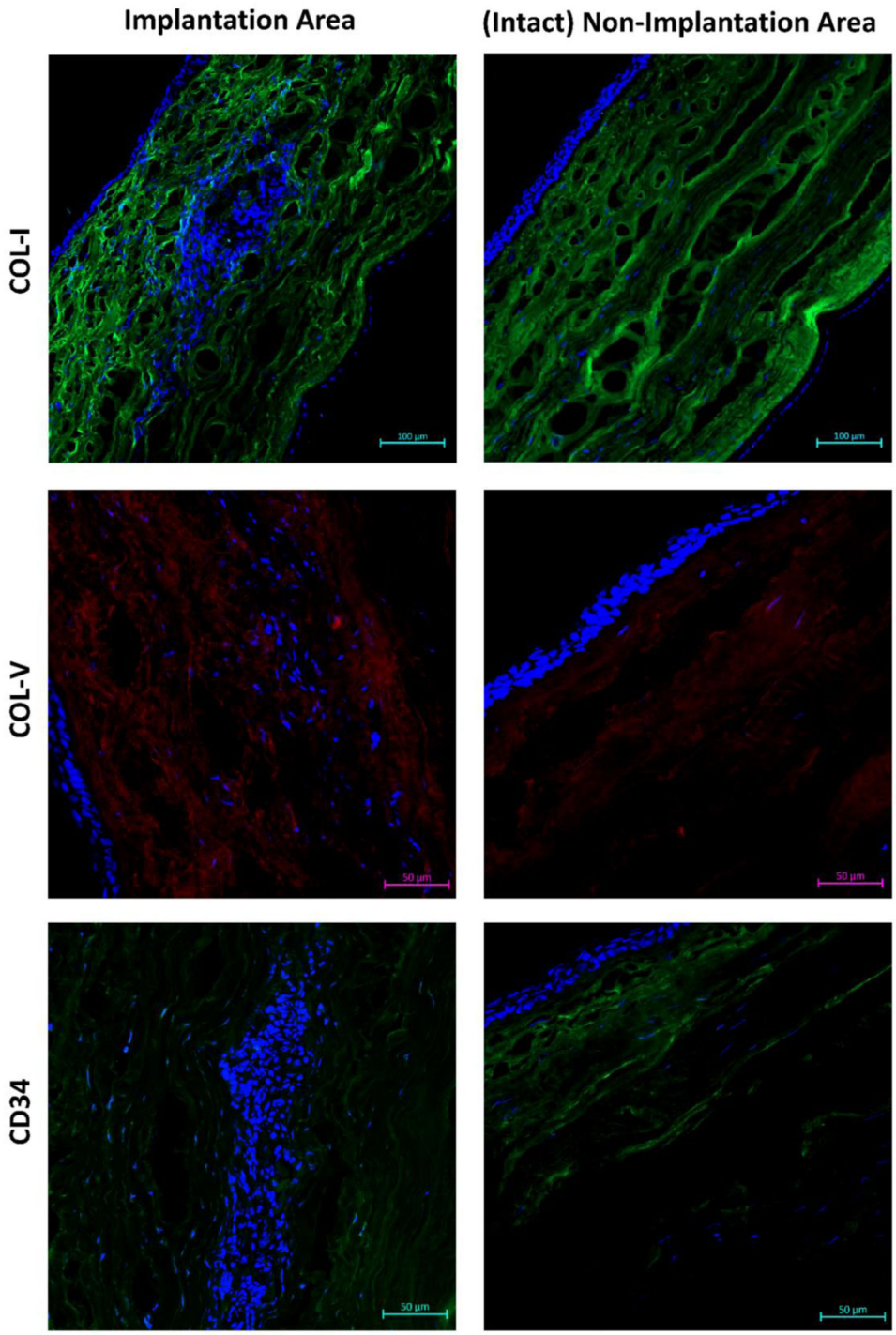

Figure 8. Confocal Laser Scanning Microscope (CLSM) images of corneal sections of implantation and non-implantation regions immunostained against COL-I (green), COL-V (red), and CD34 (green), and counterstained with DAPI for nuclei (blue). Magnifications: (COL-I) 10x; (COL-V) 20x; (CD34) 20x. Scale bars: 100 µm for COL-I, 50 µm for COL-V and CD34.

methacrylation, DM) was calculated using the MestreNova NMR analysis program according to the protocol previously published by the group.[12] Briefly, the concentrations of Gel and GelMA were normalized according to the aromatic amino acid (phenylalanine) signal located between 7.5 and 6.9 ppm in the spectrum. The integrations of the lysine methylene regions (2.95–2.80 ppm) of Gel and GelMA were obtained and the degree of methacrylation (DM) was calculated using the following equation.[12]

$$\mathrm{DM}\,(\%) = \left(1 - \frac{\text{Area of lysine methylene region of GelMA}}{\text{Area of lysine methylene region of pure gelatin}}\right) \times 100 \quad (1)$$

Preparation of 3DP Hydrogels: Cell free and cell containing artificial corneal stroma substitutes were 3D printed by EnvisionTEC printer (Gladbeck, Germany). The device was localized in a cell culture laboratory. Preprinting solution having GelMA (15%, w/v) and photoinitiator Irgacure 2959 (0.5%, w/v) was prepared in isotonic phosphate buffer (PBS, (10 mM, pH 7.4)). The solution was loaded into the print head. 3DP process was carried out using a low temperature printing unit at 20 °C, at optimized pressure and speed, and square prism samples with dimensions of 10 mm x 10 mm x 0.6 mm were produced. UV (365 nm, 1.6 J cm^{-2}, BIO-LINKTM UV Crosslinker DLX-365, Germany) was applied to both sides of the samples to stabilize them via crosslinking. Cylindrical implants were punched out from these samples using a sterile, 4 mm diameter dermal punch.

Equilibrium Water Content of 3DP GelMA Hydrogels: 3D printed hydrogels were incubated in PBS (10 mM, pH 7.4) and distilled water for 24 h at 37 °C. Then the samples were taken out and the excess liquid was very carefully removed by blotting paper, and weighed to determine the wet weight (W_w) of the samples. The samples incubated in PBS (10 mM, pH 7.4) were washed with distilled water to remove the salt on the samples (due to PBS media). In order to determine the dry weight (W_d), samples were lyophilized. The equilibrium water content (EWC) of hydrogels were calculated using the equation below:

$$EWC\ (\%) = \left(\frac{W_w - W_d}{W_w}\right) \times 100 \quad (2)$$

where W_w is wet weight and W_d is dry weight.

Enzymatic Degradation of 3DP GelMA Hydrogels: 3DP hydrogels were incubated in PBS (10 mM, pH 7.4) and distilled water for 24 h at 37 °C. The samples were then freeze dried and weighed to determine the initial weight (W_i). In order to assess the stability of 3DP and crosslinked GelMA against collagenase activity, hydrogels were incubated in PBS (10 mM, pH 7.4) containing collagenase (17.6 U mL^{-1}) for 1 and 2 h at 37 °C. As a control, GelMA hydrogels were incubated under the same conditions but without collagenase. The samples were subsequently freeze dried and weighed to determine the final weight (W_f). The degradation extent was determined gravimetrically. Enzymatic degradation level (ED) of hydrogels was calculated using the following equation:

$$ED\ (\%) = \left(\frac{W_i - W_f}{W_i}\right) \times 100 \quad (3)$$

where W_i and W_f are initial and final weights, respectively.

Mechanical Properties of GelMA Hydrogels: The mechanical resistance of the hydrogels against compression was measured using a 20 N load cell and at a speed of 1 mm min^{-1}, at room temperature (RT) (Universal Tester, Shimadzu, Japan). Samples with cells were kept in a cell growth medium until the test was performed. Samples without cells were kept in PBS containing 0.2% sodium azide. Both groups were kept at 37 °C. In order to have samples with a height suitable for mechanical testing, 4-layer samples were stacked on top of each other obtaining an average height of 3.5 mm (suitable for a compression test). Tests were applied to the hydrogels on days 1, 7, 14, and 21 of incubation. The compressive elastic modulus (E) of the samples was calculated using the initial linear region in the stress-strain plots using the following equations:

$$\text{Stress}: \ \sigma = \frac{F}{A} \quad (4)$$

$$\text{Strain}\ \varepsilon = \frac{\Delta l}{l} \quad (5)$$

$$\text{Compressive Elastic Modulus}: \ E = \frac{\sigma}{\varepsilon} \quad (6)$$

where F: Applied load, A: Cross-sectional area, l: Initial thickness, and Δl: Change in thickness.

Light Transmittance of 3DP GelMA Hydrogels: Cell free and cell loaded samples were placed in 96-well plates and placed in the growth medium and on days 0, 1, 3, 7, 14, and 21 light transmittance was measured in the range 250–700 nm, using a UV–Vis spectrophotometer (Multiscan, Thermo Scientific, USA).

In Vitro Studies—Culture and Characterization of Human Keratocytes: Human corneal keratocyte cells at passages 5–15 were used (kind gift by Prof. Odile Damour, Banque de Cornées des Hospices Civils de Lyon, France). They were frozen in growth medium containing 15% dimethyl sulfoxide (DMSO) and stored in liquid nitrogen. After thawing the cells, they were cultured with growth medium composed of Dulbecco's Modified Eagle Medium-Ham's nutrient mixture F12 (DMEM–HAM's F12, 1:1), Newborn Calf Serum (10%), amphotericin B (1 µg mL^{-1}), penicillin (100 UI mL^{-1}), streptomycin (100 µg mL^{-1}) and bFGF (Basic Fibroblast Growth Factor, 10 ng mL^{-1}) at 37 °C in a humidified 5% CO_2 incubator. Growth media were changed every two days.

Characterization of the cells was performed through flow cytometry and immunocytochemistry to determine whether keratocytes preserved their phenotypes. Cell surface antigens (Alexa Fluor 488 conjugated CD34 and CD45, APC conjugated CD73, and Alexa Fluor 647 conjugated CD90, Biolegend, USA) were studied with flow cytometer (BD Accuri C6 flow cytometer). Cells (1×10^6 cells μL^{-1}) were incubated with the antibodies presented above in FACS buffer (PBS containing 1% BSA and 0.1% sodium azide) for 30 min at RT, and then fixed in 4% paraformaldehyde (PFA) for 15 min. The cells were washed with FACS buffer and centrifuged, and the resulting pellet was suspended in FACS buffer again. Isotype controls were also used to distinguish specific antibody signal from non-specific background signal.

Immunocytochemistry examinations of the cells were conducted with a confocal laser scanning microscope (CLSM, Zeiss, Germany) for ALDH1A1 and lumican proteins found in human keratocytes. Keratocytes were seeded in 24-well cell culture plates at 5000 cells $well^{-1}$, cultured at 37 °C for 2 days, and fixed at RT with 4% PFA. Before antibody staining, cell membranes were permeabilized with 0.1% Triton X-100 treatment at RT for 10 min. Then, the cells were incubated with blocking solution of 1% BSA (30 min, 37 °C). Primary antibodies anti-human ALDH1A1 (mouse; clone 5G9E6C9, dilution factor, 1:60) and anti-human lumican (rabbit; clone JE11-45, dilution factor, 1:150) were prepared in 0.1% BSA and cells were incubated in the primary antibody solutions at +4 °C overnight. After washing with PBS, the cells were incubated with secondary antibodies conjugated with Alexa Fluor-488 and Alexa Fluor-555 at 37 °C for 1 h. Then, the cells were washed with PBS, nuclei were counterstained with DAPI (1:5000) for 15 min at RT and examined with CLSM.

In Vitro Studies—Preparation of Keratocyte Loaded GelMA Hydrogels: In order to prepare cell loaded hydrogels, human corneal keratocytes were lifted with 0.5% (w/v) trypsin, centrifuged at 3000 rpm for 5 min, and the cell number was determined with NucleoCounter (Chemo-Metec, Denmark). Cells (1×10^6) were added into GelMA solution (15% w/v) prepared in growth medium (DMEM HAM's F12, 1:1 containing 10% fetal calf serum, 1% penicillin/streptomycin, 10 ng mL^{-1} bFGF and 0.4% amphotericin). The cell carrying GelMA solution was loaded into printer heads, and the process used in cell-free printing was repeated. The cell carrying cornea equivalents (3DBP) were washed 3 times with growth medium and kept in an incubator (37 °C, 5% CO_2) for in vitro studies.

In Vitro Studies—Cell Viability: The viability of keratocytes loaded in the hydrogels was determined by Live/Dead Cell Viability test on days 3, 7, 14, and 21. For this process, the growth medium was removed, and the samples were kept at RT for 30 min with calcein AM (2 µM, in PBS) and ethidium homodimer 1 (4 µM, in PBS). Then, the samples were washed with PBS and examined with a CLSM (Zeiss LSM 800). Live (calcein stained, green) and dead cells (ethidium homodimer-1 stained, red) were counted using the NIH ImageJ program and the cell viability rate within the hydrogels was calculated according to the equation given below.

$$\textit{Cell viability}\ (\%) = \frac{\textit{Live cells}}{\textit{Live} + \textit{Dead cells}} \times 100 \quad (7)$$

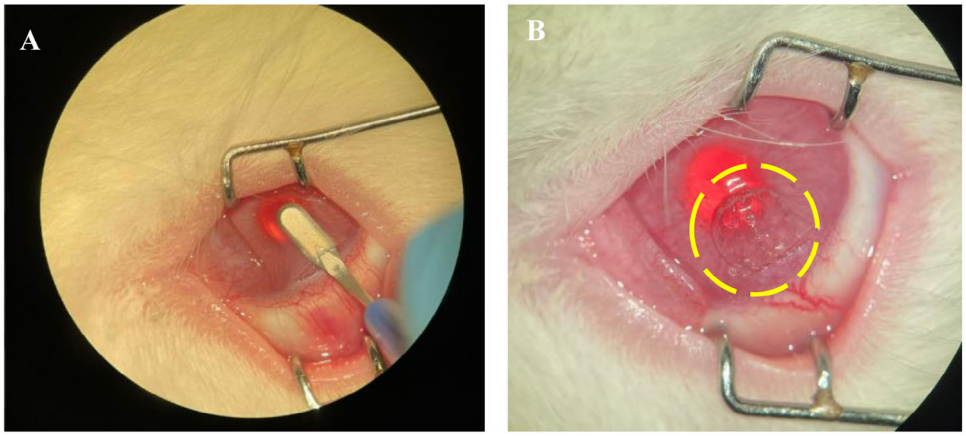

Figure 9. New Zealand White Rabbit in vivo applications: A) Linear dissection of the stroma and formation of the pockets for the implants, B) Implant within the corneal pocket.

In Vivo Tests on Rabbit Model: The number of adult rabbits to be tested in the study was calculated using ANOVA power analysis with 80% power (1-β), 0.05 statistical significance (α), and 0.69 effect size (f), and it was determined that 6 rabbits were required for each group. Ethical approval was obtained for the use of laboratory animals by the Research Ethics Commission for animal experiments (ACU-HADYEK-2022/22). A total of 18 New Zealand White rabbits were planned in this study but 2 died during surgeries and therefore control group consisted of 4 rabbits instead of 6. Cell-loaded hydrogels were produced as explained above using the 3DBP method.

Groups in the study:

Group 1 (C): Control group: Group with no surgical procedure

Group 2 (S): Sham group: Group with only a lamellar incision of the corneal layer

Group 3 (CL): Implant group: Group with cell-loaded implants

All samples were incubated in growth medium (DMEM HAM's F12, 1:1 containing 10% fetal calf serum, 1% penicillin/streptomycin, 10 ng mL^{-1} bFGF and 0.4% amphotericin) (37 °C, 5% CO_2). In order to avoid the risk of dropping samples during surgery or disrupting sterility for some reason, ≈20 implants were produced and kept ready in the operation room.

All rabbits scheduled for lamellar incision surgery on their corneas were anesthetized with general anesthesia. The necessary sterilization procedures inside and around the eye was made. A perpendicular subtotal, nonpenetrating incision was made on the superficial part of the cornea using a 45° blade on the cornea. Then, with the help of the crescent blade, the lamellar incision was applied with horizontal movements toward the central cornea, and a corneal pocket was created at the proximal part of the interface, 0.5 mm wider than the planned implant (**Figure 9**A). Afterward, the implant (dia 4 mm, thickness 600 µm) was placed from the proximal end of the corneal pocket toward the center using the dalk disector forceps, applying minimal pressure. The implant is completely placed in the corneal pocket, including the proximal part of the implant. The implants did not come out after they were placed, and therefore the operation was completed without any stitches. The hydrogels were observed to maintain their shape, integrity, and transparency at the lamellar incision interface after implantation (Figure 9B). All procedures except implantation were performed on rabbits in the sham group. In order to investigate the inflammation that may arise especially from the lamellar surgical incision, a lamellar incision was applied to the corneas of the rabbits in this group and a pocket was created in the stroma.

No procedure was applied to the Control group.

Netildex eye drops were applied to the rabbits whose corneas underwent lamellar incision for 1 week after the operation.

Monitoring of Rabbits After Surgery: Rabbits were monitored for 90 days post-implantation. The first observations were made 2 days after implantation, and then every week for the first month, and every 2 weeks thereafter. Photographs were taken at all time points. At each observation, the presence of edema in the eyes, vascularization, ulcer formation, inflammation/infection formation, condition of the incision, corneal integrity after staining with sodium fluorescein (NaF), rejection of the implant, color, and condition of the implant were checked. In addition to these, tear formation was determined numerically by applying the Schirmer's test at each observation, and tear formation was assessed, and compared with those of Sham and Control groups.

Histopathological Examinations: The rabbits were terminated after 90 days of operation and the corneas were removed. They were frozen at −80 °C after embedding in OCT (Optimal Cutting Temperature) solution. Sections (5 µm thick) were obtained using a cryomicrotome. In order to examine the general structure of the cornea, tissue response and integration of implant within the tissue, cryosections were stained with Hematoxylin-Eosin and examined with a light microscope. In addition, implant-tissue integration was investigated in detail in cell-loaded 3DBP implant group by doing immunohistochemistry against ECM molecules like collagen type I and collagen type V. Moreover, the presence of keratocytes around and in the implant was assessed through the expression of keratocyte marker CD34. First, samples were fixed with 4% paraformaldehyde for 10 min. The sections were treated with 100 mM glycine for 15 min at RT. Following wash with PBS, the sections were incubated with 0.1% Triton X-100 in PBS (PBST) for 10 min at RT to permeabilize cell membranes. Then, the samples were incubated in blocking solution of 1% BSA (in PBST) for 30 min at 37 °C. Primary antibodies for collagen type I (1:2000), collagen type V (1:50), and CD34 (1:100) were prepared in 0.1% BSA and the sections were incubated in the antibody solution at +4 °C overnight. After washing with PBS, the sections were incubated with secondary antibodies conjugated with FITC (1:250) and Alexa Fluor-555 (1:200) at 37 °C for 1 h, and following PBS wash the sections were counterstained with DAPI (1:5000) for 10 min at RT. The tissue sections were examined with a CLSM (LSM 900, Zeiss, Germany).

Acknowledgements

The authors express their gratitude to Health Institutes of Türkiye for the financial support for the project and scholarship for D.B. and A.A. through project 11745, to Acibadem Mehmet Ali Aydinlar University (ACU) for the use of the facilities and the ACU-Experimental Animals Application and Research Center (ACU-DEHAM) and to METU BIOMATEN Center of Excellence in Biomaterials and Tissue Engineering for the use of the facilities.

Conflict of Interest

The authors declare no conflict of interest.

Data Availability Statement

The data that support the findings of this study are available from the corresponding author upon reasonable request.

Keywords

3D printing, biomaterials, corneal stroma, hydrogels, tissue engineering

Received: November 30, 2024
Revised: March 5, 2025
Published online: March 27, 2025

[1] T. V. Chirila, C. R. Hicks, P. D. Dalton, S. Vijayasekaran, X. Lou, Y. Hong, A. B. Clayton, B. W. Ziegelaar, J. H. Fitton, S. Platten, *Prog. Polym. Sci.* **1998**, *23*, 447.
[2] N. J. Fullwood, *Structure* **2004**, *12*, 169.
[3] J. A. West-Mays, D. J. Dwivedi, *Int. J. Biochem. Cell Biol.* **2006**, *38*, 1625.
[4] C. J. Connon, *Procedia Eng.* **2015**, *110*, 15.
[5] R. Viitala, V. Franklin, D. Green, C. Liu, A. Lloyd, B. Tighe, *Acta Biomater.* **2009**, *5*, 438.
[6] K. Laattala, R. Huhtinen, M. Puska, H. Arstila, L. Hupa, M. Kellomäki, P. K. Vallittu, *J. Mech. Behav. Biomed. Mater.* **2011**, *4*, 1700.
[7] P. Fagerholm, N. S. Lagali, K. Merrett, W. B. Jackson, R. Munger, Y. Liu, J. W. Polarek, M. Söderqvist, M. Griffith, *Sci. Transl. Med.* **2010**, *2*, 46ra61.
[8] M. M. Islam, O. Buznyk, J. C. Reddy, N. Pasyechnikova, E. I. Alarcon, S. Hayes, P. Lewis, P. Fagerholm, C. He, S. Iakymenko, *NPJ Regen. Med.* **2018**, *3*, 2.
[9] T. Mimura, S. Amano, S. Yokoo, S. Uchida, S. Yamagami, T. Usui, Y. Kimura, Y. Tabata, *Mol. Vision* **2008**, *14*, 1819.
[10] M. Rafat, F. Li, P. Fagerholm, N. S. Lagali, M. A. Watsky, R. Munger, T. Matsuura, M. Griffith, *Biomaterials* **2008**, *29*, 3960.
[11] J.-Y. Lai, Y.-T. Li, C.-H. Cho, T.-C. Yu, *Int. J. Nanomed.* **2012**, *7*, 1101.
[12] C. Kilic Bektas, V. Hasirci, *J. Tissue Eng. Regener. Med.* **2018**, *12*, e1899.
[13] B. Kong, Y. Chen, R. Liu, X. Liu, C. Liu, Z. Shao, L. Xiong, X. Liu, W. Sun, S. Mi, *Nat. Commun.* **2020**, *11*, 1435.
[14] A. Isaacson, S. Swioklo, C. J. Connon, *Exp. Eye Res.* **2018**, *173*, 188.
[15] F. Wang, W. Shi, H. Li, H. Wang, D. Sun, L. Zhao, L. Yang, T. Liu, Q. Zhou, L. Xie, *Ocul. Surf.* **2020**, *18*, 748.
[16] S. Ulag, E. Ilhan, A. Sahin, B. K. Yilmaz, N. Ekren, O. Kilic, F. N. Oktar, O. Gunduz, *Eur. Polym. J.* **2020**, *133*, 109744.
[17] D. L. Williams, B. M. Wirostko, G. Gum, B. K. Mann, *Invest. Ophthalmol. Visual Sci.* **2017**, *58*, 4616.
[18] L. Koivusalo, M. Kauppila, S. Samanta, V. S. Parihar, T. Ilmarinen, S. Miettinen, O. P. Oommen, H. Skottman, *Biomaterials* **2019**, *225*, 119516.
[19] Y.-P. Lee, H.-Y. Liu, P.-C. Lin, Y.-H. Lee, L.-R. Yu, C.-C. Hsieh, P.-J. Shih, W.-P. Shih, I.-J. Wang, J.-Y. Yen, *Colloids Surf. B Biointerfaces.* **2019**, *175*, 26.
[20] B. He, J. Wang, M. Xie, M. Xu, Y. Zhang, H. Hao, X. Xing, W. Lu, Q. Han, W. Liu, *Bioact. Mater.* **2022**, *17*, 234.
[21] Y. Han, C. Li, Q. Cai, X. Bao, L. Tang, H. Ao, J. Liu, M. Jin, Y. Zhou, Y. Wan, Z. Liu, *Biomed. Mater.* **2020**, *15*, 035022.
[22] H. Jiang, Y. Zuo, L. Zhang, J. Li, A. Zhang, Y. Li, X. Yang, *J. Mater. Sci. Mater. Med.* **2014**, *25*, 941.
[23] W. Schuurman, P. A. Levett, M. W. Pot, P. R. van Weeren, W. J. Dhert, D. W. Hutmacher, F. P. Melchels, T. J. Klein, J. Malda, *Macromol. Biosci.* **2013**, *13*, 551.
[24] D. N. Heo, W.-K. Ko, M. S. Bae, J. B. Lee, D.-W. Lee, W. Byun, C. H. Lee, E.-C. Kim, B.-Y. Jung, I. K. Kwon, *J. Mater. Chem. B.* **2014**, *2*, 1584.
[25] L. E. Bertassoni, J. C. Cardoso, V. Manoharan, A. L. Cristino, N. S. Bhise, W. A. Araujo, P. Zorlutuna, N. E. Vrana, A. M. Ghaemmaghami, M. R. Dokmeci, *Biofabrication* **2014**, *6*, 024105.
[26] C. Kilic Bektas, V. Hasirci, *J. Mater. Sci. Mater. Med.* **2020**, *31*, 1.
[27] C. Kilic Bektas, A. Burcu, G. Gedikoglu, H. H. Telek, F. Ornek, V. Hasirci, *J. Biomater. Sci., Polym. Ed.* **2019**, *30*, 1803.
[28] M. Santoro, J. Navarro, J. P. Fisher, *Small Methods* **2018**, *2*, 1700318.
[29] A. Sorkio, L. Koch, L. Koivusalo, A. Deiwick, S. Miettinen, B. Chichkov, H. Skottman, *Biomaterials* **2018**, *171*, 57.
[30] C. Deng, F. Li, J. M. Hackett, S. H. Chaudhry, F. N. Toll, B. Toye, W. Hodge, M. Griffith, *Acta Biomater.* **2010**, *6*, 187.
[31] C. K. Bektas, V. Hasirci, *Biomater. Sci.* **2020**, *8*, 438.
[32] M. Zhang, F. Yang, D. Han, S.-Y. Zhang, Y. Dong, X. Li, L. Ling, Z. Deng, X. Cao, J. Tian, *Int. J. Bioprinting.* **2023**, *9*, 5.
[33] C. Peris-Martínez, M. C. García-Domene, M. Penadés, M. J. Luque, E. Fernández-López, J. M. Artigas, *J. Clin. Med.* **2021**, *10*, 4490.
[34] E. A. Boettner, J. R. Wolter, *Invest. Ophthalmol. Visual Sci.* **1962**, *1*, 776.
[35] L. Kessler, S. Gehrke, M. Winnefeld, B. Huber, E. Hoch, T. Walter, R. Wyrwa, M. Schnabelrauch, M. Schmidt, M. Kückelhaus, *J. Tissue Eng.* **2017**, *8*, 2041731417744157.
[36] H. Miyake, Y. Kawano, H. Tanaka, A. Iwata, T. Imanaka, M. Nakamura, *Clin. Ophthalmol.* **2016**, *10*, 879.
[37] N. Brott, M. Zeppieri, Y. Ronquillo, *StatPearls*, StatPearls Publishing, Treasure Island, FL **2024**.
[38] J. M. Anderson, A. Rodriguez, D. T. Chang, *Semin. Immunol.* **2008**, *20*, 86.
[39] S. E. Wilson, *Exp. Eye Res.* **2020**, *201*, 108272.
[40] J. W. Nichol, S. T. Koshy, H. Bae, C. M. Hwang, S. Yamanlar, A. Khademhosseini, *Biomaterials* **2010**, *31*, 5536.